

# TOWARD A PERMEABILITY PREDICTION TOOL FROM MULTISCALE MODELLING OF TRANSVERSE CRACKS ACCUMULATION IN LAMINATES

Jean Vereecke<sup>1,3</sup>, Christophe Bois<sup>1</sup>, and Jean-Christophe Wahl<sup>1</sup>, Bruno Desmars<sup>2</sup>, Florian Lavelle<sup>3</sup>

<sup>1</sup> UMR 5295 I2M, CNRS, Université de Bordeaux, Bordeaux INP, Arts & Métiers Paris-Tech  
351 Cours de la Libération, F-33400 Talence, France

<sup>2</sup> Structure composite, ArianeGroup SAS, Saint-Médard-en-Jalles, France

<sup>3</sup> Direction des Lanceurs, Centre National d'Études Spatiales (CNES) Paris, France

**Keywords:** Multi-scale modelling, Transverse cracking, Permeability, Cryogenic temperatures

## ABSTRACT

In a context of massive investments in cryogenic propellant storage, full linerless composite tanks are a technological challenge. Their mass-to-performance ratio makes them a high potential material in aerospace industry, but their permeability constitutes a limiting factor. Indeed, the pressurization of the tank and cryogenic temperatures generate matrix damages that coalesce and form privileged leakage paths. In order to master the permeability of a structure, a particular attention must be paid on damage prediction. The large number of parameters that influence the damage behaviour of the composite makes an experimental characterization tedious while virtual tests could complete the data. In this paper, a methodology is proposed to predict the crack accumulation in a single ply and identify fracture properties at a microscale. Then through a homogenization method, a mesoscale model is developed by considering the crack rate as a damage variable. It allows to evaluate the damage state of each ply according to the thermomechanical load applied. This model is adapted to industrial applications thanks to its versatility and its time calculation.

## 1 INTRODUCTION

The application of CFRP laminates to the structures of cryogenic linerless propellant tanks has been widely attempted in order to drastically reduce the weight of space launch vehicles. However, recent studies suggest that the conventional high-performance composites used in these tanks are prone to matrix cracking when exposed to extreme thermomechanical loads [1], [2]. These damage mechanisms are critical regarding permeability since this can lead to detrimental propellant leakage if left unchecked. Therefore, it is necessary to develop reliable guidelines for using CFRP laminates in cryogenic propellant tanks in order to avoid fuel and gas leakage and mitigate damage tolerance.

The strong relationship between the damage state of the composite and its permeability imposes a good understanding of the crack accumulation in every ply. Mechanical tests alone cannot identify the cracking process of a composite laminate due to the combination of the material (heterogeneity of the microstructure, local defects), the laminate (ply thicknesses and orientations), the internal pressure, and the residual thermal stresses [3]. Virtual tests, such as finite element simulations, can be used to observe the real morphology of the damage in a representative cell of the material. These simulations can evaluate the influence of some parameters on the damageable behavior of the composite and evaluate the influence of damage on the ply properties.

In this paper a methodology is proposed to model the crack accumulation in a single ply using Finite Fracture Mechanics (FFM). This model is used to discuss the relevance of the method, to identify fracture properties through an inverse identification and to observe the behavior of the ply while cracks accumulate. This model is unsuitable for industrial applications because of its scale and its time calculation. It is then transposed at a mesoscopic model thanks to a bridge between scales built by Ladevèze and Lubineau [4]. It provides damage rates for each ply according to the thermomechanical load applied. This constitutes the first step for the prediction of leakage paths.

## 2 EXPLICIT MODELLING OF CRACKS ACCUMULATION

### 2.1 Choice of method

The modelling of cracks accumulation in a 90°-ply has been widely studied in literature. Multiple methods have been proposed at the crack scale. The microscopic scale is appropriated for the simulation of the crack initiation or fiber-matrix decohesion [5], [6]. The representation of cracks can be done explicitly using cohesive-zone model [7], [8], or finite fracture mechanics [9] or by remeshing using eXtended Finite Element Method (XFEM) [10]. Since almost a hundred of cracks are created perpendicularly to the load direction, the XFEM is not relevant, a comparison between CZM and FFM has shown the relevance of the last one on this particular damage process [11].

A model based on Finite Fracture Mechanics (FFM) is proposed for explicitly modeling transverse cracking at the mesoscopic scale. This model is based on the work of Irwin [12], who developed the concepts of Griffith [13], Inglis [14] and Westergaard [15]. Irwin proposed a criterion for rupture based on surface energy, which states that a crack is created when the energy released by the sample per unit area exceeds a critical value known as the critical energy release rate. Leguillon [16] showed that this criterion should be combined with a stress criterion in order to explain Parvizi's experimental results [17]. Cornetti et al. [18] proposed an integral formulation on the crack surface which couples the two criteria to find a unique solution according to the cracked surface and the loading level. This double criterion allows the study of configurations with stress concentrations, and is able to reproduce the influence of the ply thickness on the transverse cracking threshold (see Fig 1).

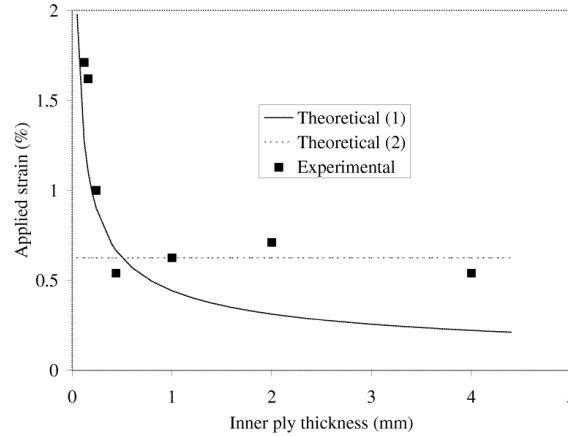


Figure 1: Theoretical (1) denotes the energy criterion, theoretical (2) the stress criterion, they are compared to Parvizi's [17] results [16]

### 2.2 Methodology

The following methodology is taken from previous work [11]. The model presented in Fig. 2 is used to determine the load at which a single potential crack is created, with respect to the fracture criterion. The potential crack is defined by its presupposed crack path. At first, it assumes perfect interfaces, infinitely rigid and without thickness. The stress criterion is calculated using an averaged Hashin mixed-mode formula (equation (2)) which generally provides good agreement with experimental results [19]:

$$\frac{1}{a} \int_a \left[ \left( \frac{\sigma_{nn}(a)}{\sigma_{nn}^c(a)} \right)^2 + \left( \frac{\sigma_{tt}(a)}{\sigma_{tt}^c(a)} \right)^2 \right] da \geq 1 \quad (2)$$

The energetic criterion is checked by calculating the energy dissipated by the crack. The potential crack is open by disactivating the interface constraints and the internal energy is progressively reduced. The

ratio between the energy released and the surface created gives the energy release rate  $G$ . As states by FFM, the energy criterion is checked when equation (1) is checked:

$$\int_{\delta a} [G(a) - G_T^c(a)] da \geq 0 \quad (1)$$

The mode mixity is evaluated by successively opening the crack in purely mode I or mode II and Benzeggagh-Kenane mixed mode equation [20] is used to calculate the critical energy release rate  $G_T^c$ .

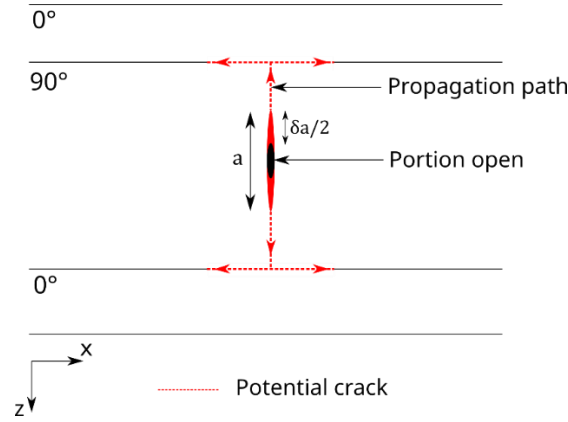


Figure 2: Proposed propagation path for a mono-cracked cell

The two criteria become valid sequentially, depending on the thickness of the ply. Indeed, a thick ply stores quickly a large amount of energy, therefore the energetic criterion is checked at first. For a thin ply, the limit stress is usually checked at first, making the energetic criterion driving the process. The influence of the ply thickness observed by Parvizi [17] is well reproduced.

### 2.3 Multi-cracked cell

The cracking kinetics of the experimentally obtained results show a slow and progressive rate of evolution at the start, which may be the result of lower local cracking thresholds that can be represented as defects or weaker areas in the ply. To consider material variability, potential cracks are periodically distributed in the multi-crack geometry presented in Fig 3.

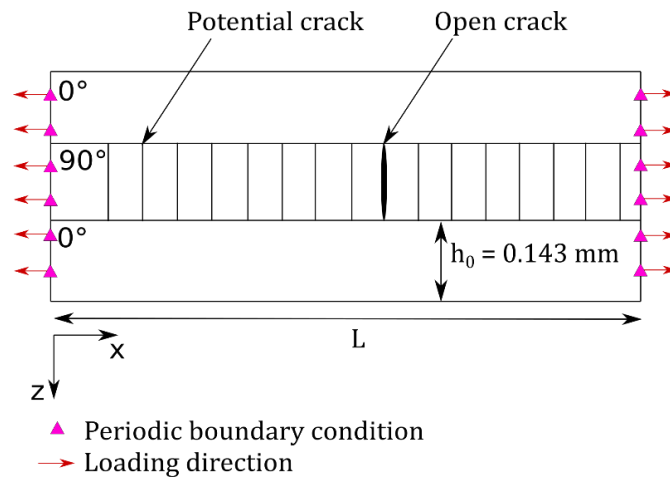


Figure 3: Geometry of the multi-cracked cell associated to a [0/90/0] laminate

$$P(x) = \frac{(x - x_{min})^\alpha (x_{max} - x)^\beta}{\int_{x_{min}}^{x_{max}} (x - x_{min})^\alpha (x_{max} - x)^\beta dx} \quad (3)$$

A probabilistic Weibull-type distribution (equation (3)), as suggested by [8], [21]–[23], is used where, parameters  $x_{min}$  and  $x_{max}$  are the limit values,  $\alpha$  and  $\beta$  are the shape and scale parameters. Previous work [11] demonstrated that 250 potential cracks over 20mm length provide acceptable results. A set of 250 values is extracted from the crack property distributions and distributed to all potential cracks along the ply.

## 2.4 Results

For each potential crack in the ply, the maximum onset crack strain of both criteria is computed. The one with the lowest value is then used to initiate the crack. Elastic calculations are necessary to determine the onset crack strain for each criterion and each ply. As the damage progresses, the onset crack strain is recomputed at each new damage state. The progression of the simulation is based on damage increments instead of load increments. The reproduction of experimental results presented in Figure 3 has been performed using fracture properties from Table 2.

	$\sigma$	$G$
$x_{min}$	63 MPa	0.063 J/mm <sup>2</sup>
$x_{max}$	113 MPa	0.245 J/mm <sup>2</sup>
$\alpha$	2.8	4.5
$\beta$	5.6	0.25

Table 2: Fracture properties distribution parameters identified

The relevancy of the Finite Fracture Method (FFM) is demonstrated by its successful simulation of the kinetics for the intermediate ply thickness, which was not used for the parameter identification. The three phases of the kinetics are observed: low rate at the start, a nearly constant rate, and saturation before the laminate failure (which was not observed for the thinner ply).

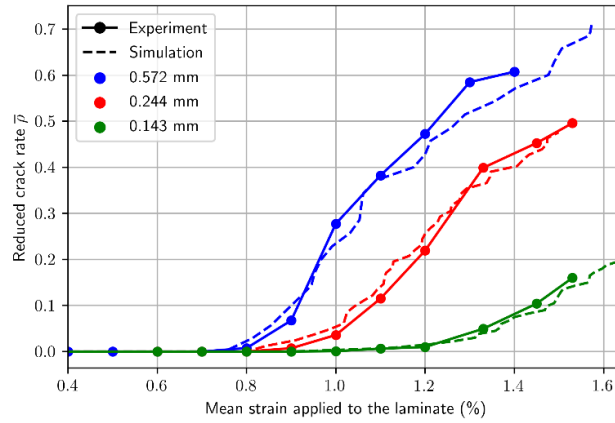


Figure 3: Cracking kinetics – Experimental and numerical results

## 3 TRANSITION FROM MICRO TO MESO-SCALE

The explicit modelling of transverse cracks accumulation is not adapted to industrial applications. Full size structures would imply a huge number of potential cracks that would increase the time calculation in a combinatorial way. A mesoscopic model, that describe the damage state of each ply with homogeneous damage variables is more appropriate. The methodology exposed in this section is based on a homogenization method proposed by Huchette [24] and Bois [25] through a bridge between micro and meso-scale established by Ladeveze and Lubineau [4]. This work has been done on a mono-cracked periodic cell in which Laeuffer included material variability and non-local corrections [26]. The previous

model is used to include the local behavior of the cracks, to identify material variability and to identify the effect of the damage accumulation on the ply stiffness and strength using a multi-cracked cell.

### 3.1 Homogenization method

The homogenization is performed to determine the influence of damage state of a ply on its elastic properties. Experimentally, in a [0/90/0] cross-ply laminate, the stiffness of the plies at 0° masks the loss of stiffness of the 90°-ply and makes the experimental measurement difficult. Numerically, it consists in the calculation of the equivalent stress of the 90°-ply when it is subjected to an elementary loading, at increasing damage levels. In other words, the stiffness tensor allowing a healthy ply to have the same homogeneous stress as the damaged ply is calculated. The equivalent stiffness tensor of the damaged ply  $\bar{\bar{C}}_{90}$  is deduced from the homogenized stiffness tensor of the laminate  $\bar{\bar{C}}_H$  by a stress equivalence (equations 4-6). For this purpose, a series of finite element calculations is performed on the cell by imposing various strain states  $\bar{E}$  and the average stress  $\bar{\Sigma}$  on this cell is recovered. Since:

$$\bar{\Sigma} = \bar{\bar{C}}_H : \bar{E} \quad (4)$$

And:

$$\bar{\bar{C}}_H = \frac{h_{90}\bar{\bar{C}}_{90} + 2h_0\bar{\bar{C}}_0}{h_{90} + 2h_0} \quad (5)$$

It gives:

$$\bar{\bar{C}}_{90} = \bar{\bar{C}}_H + 2 \frac{h_0(\bar{\bar{C}}_H - \bar{\bar{C}}_0)}{h_{90}} \quad (6)$$

The stiffness tensor can then be inverted to obtain the equivalent compliance tensor  $\bar{\bar{S}}$  of the damaged ply. For in-plane stresses, the compliance tensor  $\bar{\bar{S}}$  of the 90°-ply is written:

$$\bar{\bar{S}} = \begin{bmatrix} S_{11} & S_{21} & 0 \\ S_{12} & S_{22} & 0 \\ 0 & 0 & S_{66} \end{bmatrix} \quad (7)$$

Thus, three elementary loadings are applied to the cell, allowing to calculate by equivalence  $S_{11}$ ,  $S_{22}$  and  $S_{66}$  (see Fig 4).

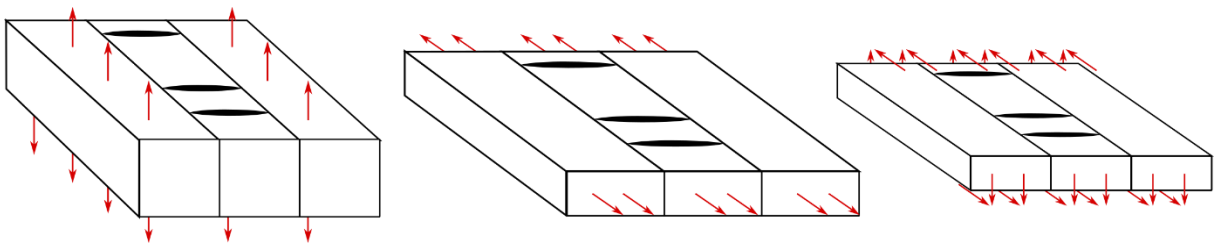


Figure 4: Strain state providing  $S_{11}$ ,  $S_{22}$  and  $S_{66}$

In our case, the explicit crack accumulation model presented above provides a cracking scenario. By reproducing the sequence of cracks created, the damage rate of the ply increases. Only the coefficients  $S_{22}$  and  $S_{66}$  are significantly influenced by the damage evolution. Thus, two elementary stresses  $\epsilon_{xx}$  and  $\epsilon_{xy}$  are applied to the cell. Figure 5 highlights the relative variation of the compliance tensor  $\Delta S_{22}/S_{22}^0$  and  $\Delta S_{66}/S_{66}^0$  with both models.

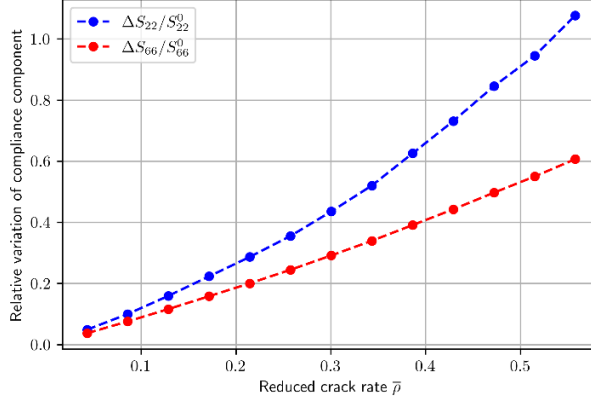


Figure 5: Definition of master curves for component 22 and 66 of the damage effect tensor

The damage effect tensor is defined as:

$$\Delta \bar{\bar{S}}(\bar{\rho}) = \bar{\bar{S}} - \bar{\bar{S}}^0 = \bar{\rho} \bar{\bar{H}}(\bar{\rho}) \quad (8)$$

In view of the evolution of the different components, the formulation of this tensor is chosen according to a quadratic form of the reduced cracking rate, that is:

$$\bar{\bar{H}}(\bar{\rho}) = \bar{\bar{H}}_1 + \bar{\rho} \bar{\bar{H}}_2 \quad (9)$$

Damage effect tensor components are identified for our study material and are used as a parameter of the damage meso-model. Each tensor of damage effect was shown to be in the following form:

$$\bar{\bar{H}}(\bar{\rho}) = \begin{bmatrix} 0 & 0 & 0 \\ 0 & h_{22}^{xy} S_{22}^0 & 0 \\ 0 & 0 & h_{66}^{xy} S_{66}^0 \end{bmatrix} \quad (10)$$

### 3.2 Evolution laws identification

#### Energy criterion

Our proposal is to establish the laws governing the evolution of the damage meso-model using strength and energy criteria, based on the methods outlined in FFM (Finite Fracture Mechanics). For the creation of the first transverse crack of the RVE, both criteria must be met. Fracture Mechanics is used to manage the increase of crack density and the propagation of microdelamination at crack tips, using the energy release rate, which explicitly accounts for the effect of ply thickness. The impact of damage on Helmholtz free energy at the meso-scale (RVE scale) is computed using the multiscale approach described in the previous section. The evolution of this free energy based on damage is defined through related thermodynamic forces in accordance with the energy criteria. A thermodynamic force  $y_{\bar{\rho}}$  associated with the reduced crack rate  $\bar{\rho}$  is defined by derivation of Helmholtz free-energy  $\Psi = \frac{1}{2} \bar{\sigma}^T : \bar{\bar{S}} : \bar{\sigma}$ .

By using the compliance tensor defined in equation 8, we obtain:

$$y_{\bar{\rho}} = \frac{\partial \Psi}{\partial \bar{\rho}} = \frac{1}{2} \left[ \bar{\sigma} : \frac{\partial}{\partial \bar{\rho}} (\bar{\bar{S}}^0 + \Delta \bar{\bar{S}}) : \bar{\sigma} \right] = \frac{1}{2} \left[ \bar{\sigma} : \frac{\partial}{\partial \bar{\rho}} (\bar{\rho} \bar{\bar{H}}(\bar{\rho})) : \bar{\sigma} \right] \quad (11)$$

$$y_{\bar{\rho}} = \frac{\partial \Psi}{\partial \bar{\rho}} = \frac{1}{2} \left[ (h_{22}^{\bar{\rho}1} + 2\bar{\rho} h_{22}^{\bar{\rho}2}) S_{22}^0 \sigma_{22}^2 + 2(h_{66}^{\bar{\rho}1} + 2\bar{\rho} h_{66}^{\bar{\rho}2}) S_{66}^0 \sigma_{66}^2 \right] \quad (12)$$

The Griffith criterion relies on the change in elastic energy that results from the formation of new crack surfaces. This change in energy must exceed the energy required for crack propagation.

$$\int_V d\Psi = G_T^c \delta a \quad (13)$$

In other words, the energy loss stored in a ply between two propagation increments, corresponds to the cracking energy multiplied by the cracked surface. The application of the Griffith criterion in the damage mesomodel finally imposes that the damage evolves if:

$$\gamma_{\bar{\rho}} - \frac{G_T^c}{h_{90}} > 0 \quad (14)$$

### Strength criterion

Based on the double criterion proposed by Leguillon and Cornetti [16], [18], the creation of a crack requires a sufficient dissipation of energy, but also a level of stress or strain higher than the allowable of the material. We define the criterion in strength as follows:

$$c = \left( \frac{\sigma_{22}}{\sigma_{22}^r} \right)^2 + \left( \frac{\sigma_{12}}{\sigma_{12}^r} \right)^2 \geq 1 \quad (15)$$

In practice, once the strain criterion is reached, since the strain of the ply is homogenized, the criterion remains valid and does not consider the local unloading induced by existing cracks. However, in a crack neighborhood, the stress field is not homogeneous. The integral formulation of the criterion, proposed by Cornetti, requires the calculation of the average stress over the entire crack path, i.e. over the thickness of the ply.

Taking the results of the explicit model, at each damage level, the average stress is calculated at the next crack and then scaled by the theoretical stress of the undamaged ply. This gives a corrected criterion  $\tilde{c}$  such that:

$$\tilde{c} = \frac{c}{c^h} \quad (16)$$

Where  $c^h$  is the homogenized strength criterion  $c^h = \left( \frac{\sigma_{22}^h}{\sigma_{22}^r} \right)^2 + \left( \frac{\sigma_{12}^h}{\sigma_{12}^r} \right)^2$  with  $\sigma_{22}$  and  $\sigma_{12}$  the theoretical transverse and shear stresses calculated for an undamaged ply and  $\sigma_{22}^r$  and  $\sigma_{12}^r$  their respective limits. The evolution of  $\tilde{c}$  is presented in Figure 6. We observe that at zero cracking rate, the corrected criterion is exactly worth the theoretical criterion, it decreases when  $\bar{\rho}$  increases since the areas in which the new cracks are created are unloaded and the stress is lower there.

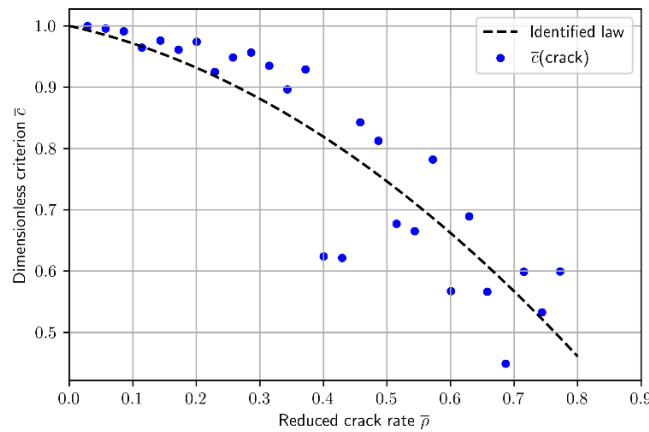


Figure 6: Dimensionless criterion  $\tilde{c}$  as a function of the reduced crack rate

The model is implemented in *Python*. The program allows for single or dual axis diagram loading, in strain or stress, so as to simulate the pressurization of a tube. Figure 7 shows the response of the model in terms of transverse cracking rate of a thick ply and a thin ply. The energy and strength criteria are shown in dotted lines. For the thick ply, since both criteria must be validated, the response of the model is driven by the weaker criterion, i.e. the strength criterion, whereas for the thin ply, the energy criterion

is limiting. In both cases, the saturation is driven by the strength criterion, which is expected considering that the saturation comes from the global unloading of the ply by the existing cracks.

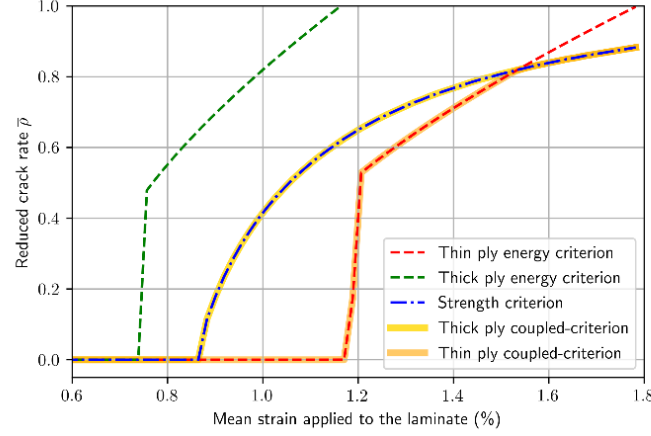


Figure 7: Model response with the double-criterion on a [0/90/0] cross-laminate for two ply thicknesses

### 3.3 Introduction of variability

Accurately predicting leakage points requires a slow initiation of cracking at the start of the process, which is influenced by defects and local variations in microstructure, such as porosities, resin clusters, or thickness variations. To model these variabilities, weaker fracture properties can be used, as demonstrated in explicit modeling. Laeuffer and Briand have proposed a method based on an average of many simulations with failure properties extracted from a phenomenological distribution.

The explicit crack accumulation model not only provides the cracking scenario but also highlights the fact that at initiation, cracks are localized at the weakest points of the ply, with low strength for thick ply and low cracking energy for thin plies. The local properties of the cracks increase with the cracking rate and balance with the local unloading induced by pre-existing cracks. Figure 8 illustrates the evolution of the critical energy release rate of the activated cracks as a function of the ply's cracking rate, with the non-monotonic behavior being characteristic of these discharges.

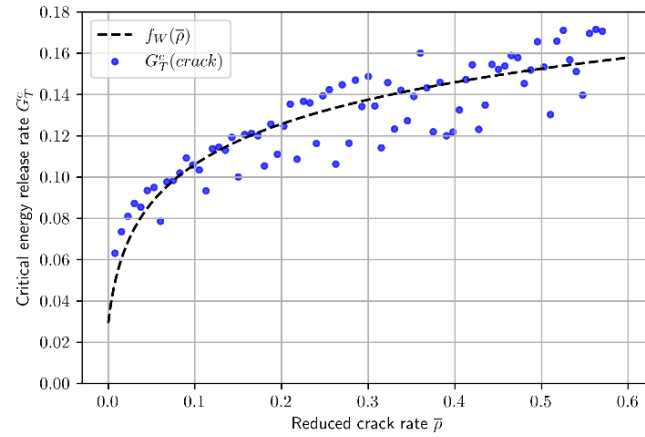


Figure 8: Evolution of critical energy release rate of created cracks with respect to the reduced crack rate of the ply



As a result, the fracture properties evolve with the damage rate, and the functions  $f_G(\bar{\rho})$  and  $f_\sigma(\bar{\rho})$  are determined by interpolating the results of the explicit model (as shown in Figure 8). Figure 9 compares the experimental results with the model predictions, noting that the laws are identified from the explicit model without any additional recalibration. The use of discrete fracture mechanics yields comparable results at both modeling scales.

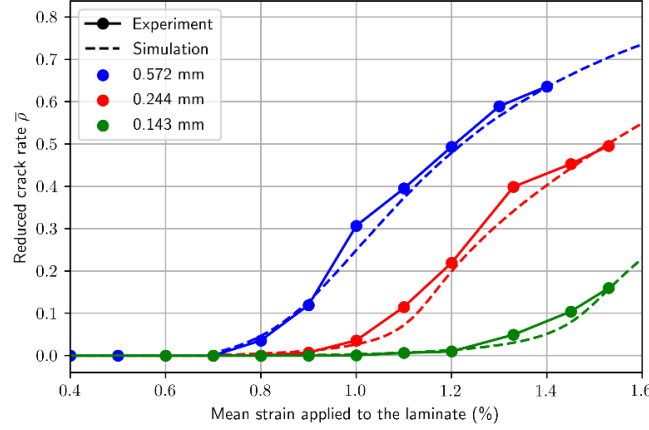


Figure 9: Model response with the double-criterion on a [0/90/0] cross-laminate for two ply thicknesses

### 3.3 Leak paths prediction

The damage prediction in every ply is necessary to study the global permeability of the structure. Many authors based their permeability prediction on the relationship between the damage state of the ply and its equivalent hydraulic conductivity. This method is inspired from Darcy's law for viscous flow of gases through porous media [27]. The methodology can be adapted in the case of crack networks that do not cross the whole laminate. If it is the case, hypotheses of porous medias are not verified and a leak model is well more appropriated. Indeed, a crack network that leads to a leak increases the permeability by a factor  $10^2$  or  $10^3$  (depending of the considered surface).

For the use of space launchers, these leaks are more likely to appear, the model described above will therefore be used to predict it. The reduced crack rate of the  $n$ -th ply  $\bar{\rho}_n$  can be easily transposed to a total crack length  $L_n$  over the surface  $S$  through the equation:  $L_n = \bar{\rho}_n * S / h_n$ . The cracks in each ply are randomly spread over the surface, considering the total length and the orientation of the ply. The graph theory is then used to represent the crack network and their connection. Each crack in a ply is a node of the graph and the link between two cracks means that they are connected. As shown on Fig. 10, the interface between two plies constitutes a bipartite graph from which the adjacency matrix  $(M)_{i,j}$  can be drawn.

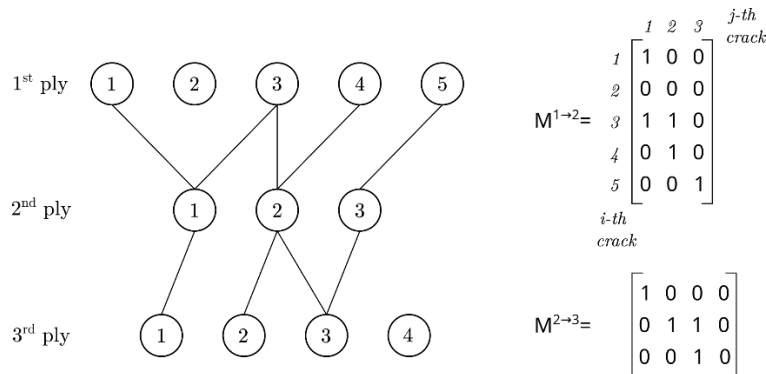


Figure 10: Example of graph used for leak paths prediction

If the  $i$ -th crack in a ply is connected to the  $j$ -th crack in the adjacent one, the component  $M_{i,j} = 1$ , otherwise the value is 0. The shape of the adjacency matrix is therefore equal to the number of cracks in both plies. This mathematical tool becomes very useful when there is a succession of interfaces. Indeed, the shape of consecutive interfaces, makes it possible to multiply the adjacency matrix. In this case, the resulting matrix shape is equal to the number of cracks in the first ply (in lines) and in the last one (in columns). The component of the matrix  $M_{i,j}$  is equal to the number of paths linking the  $i$ -th crack of the first ply with the  $j$ -th crack of the last one. By multiplying adjacency matrices from the first ply to the penultimate one, it is possible to know if cracks in this ply are effectively connected to the first one. The number of leak paths, is equal to the adjacency matrix of the last interface, considering only cracks in the penultimate ply that are connected to the first one.

Fig. 11 illustrates the progression of crack paths observed in a pressurized tubular specimen that experiences bi-axial loading. The stacking sequence of the specimen is  $[50/-15/-35_2/35_2/15/-50]$  ( $0^\circ$  being the axial direction), and the specific area under investigation spans a length of 100 mm along the circumference, corresponding to a diameter of 200 mm. Each ply of the specimen has a thickness of 0.143 mm.

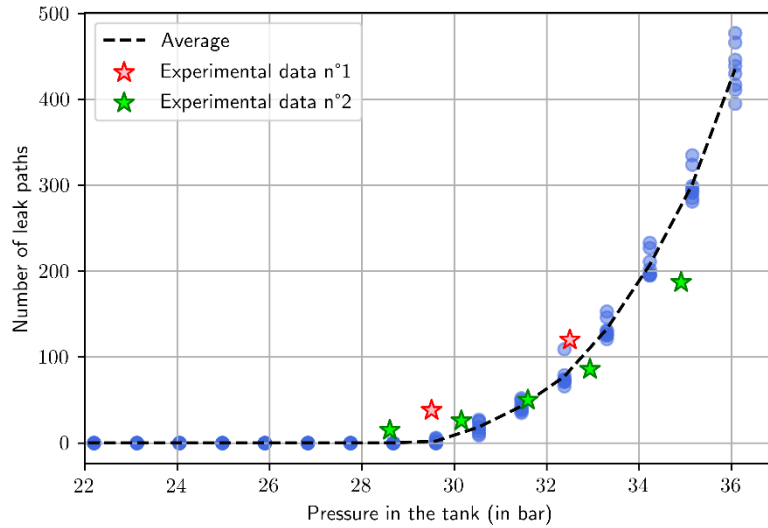


Figure 11: Evolution of the number of crack paths, prediction and experimental results

In this figure, the simulation was conducted ten times to assess the impact of random crack positions. The results indicate that the relative standard deviation (RSD) is below 6%, suggesting that the choice of random crack positions does not significantly affect the predictions. It is worth mentioning that the experimental data used in this study were obtained from a defect-free tubular specimen manufactured using automated fiber placement and controlled carefully.

#### 4 CONCLUSIONS

In this paper, an explicit mesoscopic model has been developed, based on Finite Fracture Mechanics. It highlighted damage mechanisms that drive the accumulation of transverse cracks in a single ply. The coupled criterion is able to reproduce the cracking kinetics obtained on different ply thicknesses and provides precious data such as the crack scenario and the activated fracture properties. These results have been used to identify the damage evolution laws and the variability of the mesoscopic model more adapted to industrial applications. The meso-model is able to reproduce the crack accumulation simulated with the discrete model as a function of thermomechanical conditions. It can be easily integrated in a finite element software and then used for optimization procedure thanks to its low computation time. Future works concern the study of interaction phenomena between damaged plies

and the experimental study of leaks in order to estimate the total leak associated with the number of leak paths.

## ACKNOWLEDGEMENTS

The authors would like to thank the CNES, the French space agency, and ArianeGroup for their financial support.

## REFERENCES

- [1] H. Kumazawa, T. Aoki, T. Ishikawa, et I. Susuki, « Modeling of propellant leakage through matrix cracks in composite laminates », in 42nd AIAA/ASME/ASCE/AHS/ASC Structures, Structural Dynamics, and Materials Conference nad Exhibit Technical Papers, vol. 1. 2001, p. 307-311. [En ligne]. Disponible sur: <http://www.scopus.com/inward/record.url?eid=2-s2.0-0035006595&partnerID=40&md5=04d90cccccac4d43478d15ef6b06eb60>
- [2] H. Kumazawa, T. Aoki, et I. Susuki, « Analysis and Experiment of Gas Leakage Through Composite Laminates for Propellant Tanks », *AIAA J*, vol. 41, n° 10, p. 2037-2044, 2003.
- [3] C. T. Herakovich, J. G. Gavis, et J. S. Mills, « Thermal Microcracking in Celion 6000/PMR-15 Graphite/Polyimide », in *Thermal Stresses in Severe Environments*, D. P. H. Hasselman et R. A. Heller, Éd., Boston, MA: Springer US, 1980, p. 649-664. doi: 10.1007/978-1-4613-3156-8\_40.
- [4] P. Ladevèze et G. Lubineau, « Pont entre les « micro » et « méso » mécaniques des composites stratifiés », *Comptes Rendus Mécanique*, vol. 331, n° 8, p. 537-544, août 2003, doi: 10.1016/S1631-0721(03)00130-X.
- [5] F. Naya, C. González, C. S. Lopes, S. Van der Veen, et F. Pons, « Computational micromechanics of the transverse and shear behavior of unidirectional fiber reinforced polymers including environmental effects », *Composites Part A: Applied Science and Manufacturing*, vol. 92, p. 146-157, janv. 2017, doi: 10.1016/j.compositesa.2016.06.018.
- [6] F. Danzi, D. Fanteria, E. Panettieri, et M. Palermo, « A numerical micro-mechanical study of the influence of fiber–matrix interphase failure on carbon/epoxy material properties », *Composite Structures*, vol. 159, p. 625-635, janv. 2017, doi: 10.1016/j.compstruct.2016.09.095.
- [7] F. P. Van Der Meer et C. G. Davila, « Modeling transverse cracking in laminates with a single layer of elements per ply », présenté à ECCM15-15th European Conference on Composite Materials, 2012.
- [8] D. M. Grogan, C. M. Ó Brádaigh, et S. B. Leen, « A combined XFEM and cohesive zone model for composite laminate microcracking and permeability », *Composite Structures*, vol. 120, p. 246-261, févr. 2015, doi: 10.1016/j.compstruct.2014.09.068.
- [9] I. G. García, V. Mantič, A. Blázquez, et F. París, « Transverse crack onset and growth in cross-ply [ 0 / 90 ] s laminates under tension. Application of a coupled stress and energy criterion », *International Journal of Solids and Structures*, vol. 51, n° 23-24, p. 3844-3856, nov. 2014, doi: 10.1016/j.ijsolstr.2014.06.015.
- [10] N. A. Abdullah, J. L. Curiel-Sosa, Z. A. Taylor, B. Tafazzolimoghaddam, J. L. Martinez Vicente, et C. Zhang, « Transversal crack and delamination of laminates using XFEM », *Composite Structures*, vol. 173, p. 78-85, août 2017, doi: 10.1016/j.compstruct.2017.04.011.
- [11] J. Vereecke, Bois, Christophe, Wahl, Jean-Christophe, Le Goff, Erwann, et Lavelle, Florian, « Explicit Modelling Of Matrix Damage In A Laminated Composite Comparison Between Linear Fracture Mechanic And Cohesive Zone Model », présenté à Proceedings of the 20th European Conference on Composite Materials - Composites Meet Sustainability (Vol 1-6), in Proceedings of the 20th European Conference on Composite Materials - Composites Meet Sustainability (Vol 1-6), vol. 3. Lausanne: EPFL Lausanne, Composite Construction Laboratory, 2022, p. 1159-1168. doi: 10.5075/EPFL-298799\_978-2-9701614-0-0.
- [12] G. R. Irwin, « ONSET OF FAST CRACK PROPAGATION IN HIGH STRENGTH STEEL AND ALUMINUM ALLOYS », Naval Research Lab., Washington, D.C., NRL-4763; PB-121224, mai 1956.
- [13] A. Griffith, « VI. The phenomena of rupture and flow in solids », *Phil. Trans. R. Soc. Lond. A*, vol. 221, n° 582-593, p. 163-198, janv. 1921, doi: 10.1098/rsta.1921.0006.

- [14] C. E. Inglis, « Stresses in A Plate Due To The Presence of Cracks and Sharp Corners », *Scribd*, Cambridge, 1913.
- [15] H. M. Westergaard, « Bearing Pressures and Cracks: Bearing Pressures Through a Slightly Waved Surface or Through a Nearly Flat Part of a Cylinder, and Related Problems of Cracks », *Journal of Applied Mechanics*, vol. 6, n° 2, p. A49-A53, juin 1939, doi: 10.1115/1.4008919.
- [16] D. Leguillon, « Strength or toughness? A criterion for crack onset at a notch », *European Journal of Mechanics - A/Solids*, vol. 21, n° 1, p. 61-72, janv. 2002, doi: 10.1016/S0997-7538(01)01184-6.
- [17] A. Parvizi, K. W. Garrett, et J. E. Bailey, « Constrained cracking in glass fibre-reinforced epoxy cross-ply laminates », *J Mater Sci*, vol. 13, n° 1, p. 195-201, janv. 1978, doi: 10.1007/BF00739291.
- [18] P. Cornetti, N. Pugno, A. Carpinteri, et D. Taylor, « Finite fracture mechanics: A coupled stress and energy failure criterion », *Engineering Fracture Mechanics*, vol. 73, n° 14, p. 2021-2033, sept. 2006, doi: 10.1016/j.engfracmech.2006.03.010.
- [19] Z. Hashin et A. Rotem, « A Fatigue Failure Criterion for Fiber Reinforced Materials », *Journal of Composite Materials*, vol. 7, n° 4, p. 448-464, oct. 1973, doi: 10.1177/002199837300700404.
- [20] M. L. Benzeggagh et M. Kenane, « Measurement of mixed-mode delamination fracture toughness of unidirectional glass/epoxy composites with mixed-mode bending apparatus », *Composites Science and Technology*, vol. 56, n° 4, p. 439-449, 1996, doi: 10.1016/0266-3538(96)00005-X.
- [21] E. V. Iarve, M. R. Gurvich, D. H. Mollenhauer, C. A. Rose, et C. G. Dávila, « Mesh-independent matrix cracking and delamination modeling in laminated composites », *Int. J. Numer. Meth. Engng.*, vol. 88, n° 8, p. 749-773, nov. 2011, doi: 10.1002/nme.3195.
- [22] C. Lu, R. Danzer, et F. D. Fischer, « Fracture statistics of brittle materials: Weibull or normal distribution », *Phys. Rev. E*, vol. 65, n° 6, p. 067102, juin 2002, doi: 10.1103/PhysRevE.65.067102.
- [23] J. A. Nairn, « Matrix Microcracking in Composites », in *Comprehensive Composite Materials*, Elsevier, 2000, p. 403-432. doi: 10.1016/B0-08-042993-9/00069-3.
- [24] C. Huchette, D. Lévêque, et N. Carrère, « A multiscale damage model for composite laminate based on numerical and experimental complementary tests », in *Proceedings of the IUTAM Symposium on Multiscale Modelling of Damage and Fracture Processes in Composite Materials*, in IUTAM Symposium on Multiscale Modelling of Damage and Fracture Processes in Composite Materials, vol. 135. Dolny, 2006, p. 241-248. Consulté le: 1 janvier 23apr. J.-C. [En ligne]. Disponible sur: <http://www.scopus.com/inward/record.url?eid=2-s2.0-84860766993&partnerID=40&md5=f9a777af87d9cba1b74087534270e280>
- [25] C. Bois, J.-C. Malenfant, J.-C. Wahl, et M. Danis, « A multiscale damage and crack opening model for the prediction of flow path in laminated composite », *Composites Science and Technology*, vol. 97, n° 0, p. 81-89, 2014, doi: 10.1016/j.compscitech.2014.04.002.
- [26] H. Laeuffer, B. Guiot, J.-C. Wahl, N. Perry, F. Lavelle, et C. Bois, « A model for the prediction of transverse crack and delamination density based on a strength and fracture mechanics probabilistic approach », in *ECCM17 - 17TH European Conference on Composite Materials*, Munich, Germany, 2016.
- [27] S. Roy et M. Benjamin, « Modeling of permeation and damage in graphite/epoxy laminates for cryogenic fuel storage », *Composites Science and Technology*, vol. 64, n° 13-14, p. 2051-2065, oct. 2004, doi: 10.1016/j.compscitech.2004.02.014.